

See discussions, stats, and author profiles for this publication at: <https://www.researchgate.net/publication/268522707>

# Effect of Alkyl Chain–Length on Dissociative Attachment: 1–Bromoalkanes on Si(100)–c(4×2)

ARTICLE in THE JOURNAL OF PHYSICAL CHEMISTRY C · APRIL 2012

Impact Factor: 4.77 · DOI: 10.1021/jp301773m

CITATIONS

3

READS

34

9 AUTHORS, INCLUDING:



Maryam Ebrahimi

University of Waterloo

15 PUBLICATIONS 94 CITATIONS

SEE PROFILE



Kai Huang

University of Toronto

9 PUBLICATIONS 31 CITATIONS

SEE PROFILE



Tingbin Lim

Synfuels China Ltd.

13 PUBLICATIONS 130 CITATIONS

SEE PROFILE



Iain McNab

Sheridan College (Oakville)

64 PUBLICATIONS 893 CITATIONS

SEE PROFILE

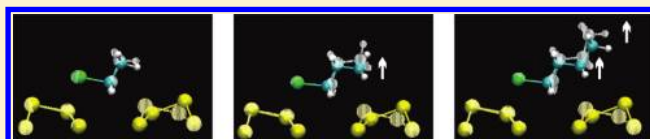
# Effect of Alkyl Chain-Length on Dissociative Attachment: 1-Bromoalkanes on Si(100)-c(4×2)

Maryam Ebrahimi,<sup>†</sup> Si Yue Guo, Kai Huang, Tingbin Lim, Iain R. McNab,<sup>‡</sup> Zhanyu Ning, John C. Polanyi,\* Mark Shapero, and Jody (S. Y.) Yang

Lash Miller Chemical Laboratories, Department of Chemistry and Institute of Optical Sciences, University of Toronto, 80 St. George Street, Toronto, Ontario, M5S 3H6 Canada

## S Supporting Information

**ABSTRACT:** Chemical reactivity as a function of chain-length was investigated for three 1-bromoalkanes on silicon. The physisorption and subsequent thermal dissociative attachment of bromoethane (EtBr), 1-bromopropane (PrBr), and 1-bromobutane (BuBr) on Si(100)-c(4×2) were examined by scanning tunneling microscopy in ultrahigh vacuum from 50 to 180 K, and interpreted by ab initio theory. These 1-bromoalkanes were found to physisorb and react exclusively over the inter-row sites of Si(100)-c(4×2), with activation barriers,  $E_a$ , increasing with alkyl chain-length:  $E_a = 343 \pm 5$  meV for EtBr,  $E_a = 410 \pm 6$  meV for PrBr, and  $E_a = 536 \pm 2$  meV for BuBr. Extensive ab initio calculations gave increasing barriers along the series:  $E_c = 317$  meV for EtBr,  $E_c = 406$  meV for PrBr, and  $E_c = 430$  meV for BuBr. On the basis of our calculated geometries, we interpret this dependence of thermal barrier on chain-length as due to the additional energy required with increasing chain-length in order to lift the alkyl chain away from the surface, in going from the initial physisorbed state to the reactive transition state. For BuBr, the measured  $E_a$  significantly exceeded the calculated value. This increase in effective barrier-height could be due to a “dynamical delay” in optimizing the configuration of the alkyl chain.



## 1. INTRODUCTION

Dissociative attachment (DA) refers here to a thermal reactive event in which a single bond of an adsorbate is cleaved and two new bonds are formed attaching the resulting fragments to the surface.<sup>1</sup> Different physisorbed states can have different reactivity via DA to the same products.<sup>2</sup> In previous work from this laboratory it was shown that the outcomes of DA were influenced by barrier-heights to chemisorption from different physisorbed states.<sup>3,4</sup> Studies from this laboratory and others have yielded knowledge of DA on both metal<sup>5</sup> and semiconductor<sup>6–9</sup> surfaces.

For any particular surface, the nature of DA is largely governed by the functional group in the prior physisorbed species. However, the effect of the side chains of adsorbate molecules on DA has rarely been examined. Side chains are adjacent to the functional group in the adsorbate molecules. For example, alkyl groups of varying structures in haloalkanes are well-known in gas-<sup>10</sup> and solution-based<sup>11</sup> reactions as side chains that alter molecular reactivity via steric<sup>11</sup> and/or electronic<sup>12</sup> effects. Here it will be shown that side chains of 1-bromoalkanes affect the reaction dynamics of DA reactions on a surface.

Using scanning tunneling microscopy (STM) we examine the physisorption and subsequent DA of a series of 1-bromoalkanes, bromoethane (EtBr), 1-bromopropane (PrBr), and 1-bromobutane (BuBr), on the Si(100)-c(4×2) surface between 50 and 180 K. These three 1-bromoalkane molecules were found to physisorb and subsequently thermally react exclusively at inter-row sites between two depressed Si-atoms

(termed “down” Si-atoms), producing atomic bromines and 1-alkyls on Si(100)-c(4×2) by way of DA in a highly localized fashion.<sup>13</sup>

Further, we found that the measured energy barriers for DA increased steadily with increasing alkyl chain-length,  $E_a = 343 \pm 5$  meV for EtBr,  $E_a = 410 \pm 6$  meV for PrBr, and  $E_a = 536 \pm 2$  meV for BuBr. These measured  $E_a$  values were largely in agreement with barriers computed by the newly implemented dispersion-force correction method within density functional theory<sup>14</sup> (the DFT-D method) which gave a priori  $E_c = 317$  meV for EtBr,  $E_c = 406$  meV for PrBr, and  $E_c = 430$  meV for BuBr; two  $E_c$  values are seen to agree closely with the measured  $E_a$ , whereas the third computed  $E_c$ , that for BuBr, is markedly lower than the measured value. This discrepancy will be discussed later in this paper.

The inclusion, in this work, of dispersion force in the DFT-D method is important in obtaining barrier heights for these DA reactions. By contrast, standard DFT calculations, as shown in earlier DA studies of similar systems from this laboratory,<sup>3,4</sup> can only be depended on for comparison of relative barrier heights on a given surface.

On the basis of our DFT-D calculations of the changes in molecular geometry occurring en route to the transition state (TS), we interpret the observed increase in barrier height with chain-length as being due to the need to overcome the

Received: February 22, 2012

Revised: April 10, 2012

Published: April 11, 2012

attraction between the alkyl chains and the silicon surface in going from the initial state (IS) to the TS. Additionally, we discuss the effect of barrier-crest location along the reaction coordinate on the requirement for “chain-lifting” prior to barrier-crossing, in this and contrasting work on metal.<sup>15</sup> In the present study we postulate a “dynamical delay” in reconfiguring the longest alkyl chain to its optimal geometry for barrier-crossing, in order to account for a significant (106 meV) discrepancy between the  $E_a$  for dissociative attachment of BuBr measured here, that substantially exceeds the computed barrier height ( $E_c$ ) to reaction. The proposed “dynamical delay” constitutes a failure of the four-carbon chain to adopt a fully optimal geometry for barrier-crossing. We calculate the small lag in raising the chain that would be required in order to explain the observed deviation of the measured  $E_a$  from the calculated  $E_c$ . Given the short time that the system spends at the barrier-crest, the existence of such a lag (which awaits confirmation by dynamical studies) appears plausible. The concept of “dynamical delay” has parallels in previous literature where it was argued that thermal reaction involves specialized (e.g., “migratory”) rather than random motion in the transition state.<sup>16–18</sup> Recent dynamical studies with moderate translational and/or vibrational excitation in the molecular reagents leave no doubt that the representative trajectories can deviate from the minimum-energy pathway for both gas-phase,<sup>19–23</sup> and gas–surface reactions.<sup>24–27</sup>

## 2. METHODS

**2.1. Experiment.** Experiments employed two separate ultrahigh vacuum (UHV) scanning tunneling microscopes (RHK300 and Omicron VT-STM), both with a base pressure less than  $6 \times 10^{-11}$  Torr. Samples of Si(100) were cut from n-type phosphorus-doped wafers with resistivity of 0.01–0.02  $\Omega$  cm. In vacuum, silicon samples were prepared by repetitive direct-current heating, following the procedure of Hata et al.<sup>28</sup> With our RHK300 STM, it was necessary to prepare Si(100) crystal on a stage precooled to 100 K; sample preparation at a stage held at 300 K usually gave  $\sim 30\%$  C-type defects.<sup>29</sup> With our Omicron STM, silicon was prepared on the manipulator arm without precooling. Then in both UHV systems, the newly prepared surface was cooled on the STM stage using either liquid nitrogen or liquid helium to achieve the required temperatures and checked by STM, showing a  $c(4 \times 2)$  reconstruction with less than 0.2% defects.

At 300 K, all adsorbate chemicals (bromoethane purchased from Sigma-Aldrich,  $\geq 99\%$  in purity; 1-bromopropane purchased from Sigma-Aldrich,  $\geq 99\%$  in purity; 1-bromobutane purchased from Alfa Aesar,  $> 98\%$  in purity) were colorless liquids and subject to 7–8 freeze–pump–thaw cycles, before being admitted into vacuum chamber through a leak valve for background dosing. The surfaces subjected to molecular exposure were checked by STM, showing a typical coverage of  $\sim 0.1$ – $5\%$  molecule per Si-dimer. Tungsten STM tips were made by a 4.5–9 V direct-current etch in 3 M NaOH solution. All STM images were recorded in the constant-current mode and processed with XPMPro 2.0.0.0. Imaging biases refer to the silicon sample bias with respect to the grounded STM tip.

**2.2. Theory.** Density functional theory (DFT) calculations, and also semiempirical DFT-D calculations that included van der Waals interactions, were made with the Vienna Ab-initio Simulation Package (VASP),<sup>30,31</sup> installed at the SciNet supercomputer.<sup>32</sup> DFT calculations were made using the Perdew–Burke–Ernzerhof generalized-gradient approximation

(PBE-GGA) for exchange-correlation potentials,<sup>33</sup> the projector augmented waves (PAW) method,<sup>34,35</sup> and a plane-wave basis set with an energy cutoff of 450 eV. Final calculations were made with the DFT-D method, in which dispersion effects are taken into account using Grimme’s method,<sup>14</sup> and the final geometries and corresponding energies should be more accurate than those from the standard DFT calculations.

Throughout this study we used a slab model of  $\text{Si}_{112}\text{H}_{32}$  with a  $c(4 \times 2)$  periodicity in a  $4 \times 4$  supercell (supercell size:  $15.361\ 25\ \text{\AA} \times 15.361\ 25\ \text{\AA} \times 30.000\ 00\ \text{\AA}$ ). The slab consisted of seven layers of Si-atoms with the bottom terminated by 32 H-atoms. The adsorbate molecules were placed on the top face of the slab. The bottom two silicon layers were frozen and then all other atoms were fully relaxed until the net force on each atom was less than 0.02 eV/ $\text{\AA}$ . The minimum energy pathways (MEPs) for DA of all three 1-bromoalkanes were determined using the climbing image nudged elastic band (CI-NEB) method<sup>36</sup> that locates the exact saddle points of the reactions.

For both DFT and DFT-D calculations, the surface Brillouin zone was sampled using a  $2 \times 2 \times 1$  k-mesh, and calculations were performed without spin-polarization. We tested the convergence of our results with a  $3 \times 3 \times 1$  k-mesh or with spin-polarization applied, and found a difference of only 7 meV in the relative energies (e.g., heat of adsorption, barrier height) for the worst case. The calculated geometries were rendered using VMD.<sup>37</sup>

We also investigated the effects of quantum zero-point energies on the computed barrier heights using the dynamical matrix method of Henkelman et al.<sup>38</sup> The zero-point energy corrections were found to only reduce the DA barriers slightly ( $\sim 40$  meV) and do not affect the calculated barrier differences along the concerned 1-bromoalkane series that are the main interest of this work. See Supporting Information for details.

## 3. RESULTS

**3.1. Experiment.** **3.1.1. Physisorption.** Physisorption and subsequent DA reactions of EtBr, PrBr, and BuBr were studied at temperatures between 50 and 180 K. At these temperatures the flipping motion of Si-dimers was “frozen out”, giving a buckled  $c(4 \times 2)$  reconstruction.<sup>39</sup> As is well-known, buckled Si dimers transfer electron density from the “down” Si-atom to the “up” Si-atom.<sup>40</sup> This is evident in a typical empty-state STM image shown in Figure 1a. In this image recorded at 100 K,<sup>41</sup> the “down” Si-atoms imaged bright while the “up” Si-atoms imaged dark. This is understood by the electron density transfer which causes “down” Si-atoms to be slightly positively charged and hence more accessible to tunneling electrons from the STM tip (hence bright) than “up” Si-atoms for which the converse applies.

Upon exposure of the cold Si(100) surface to 1-bromoalkanes individually, new bright features were observed that we assign as physisorbed 1-bromoalkanes. As indicated by arrows in Figure 1b–d, these physisorbed 1-bromoalkanes were symmetric both along and across dimer row direction (although occasionally appearing fuzzy, see Supporting Information), and exclusively at inter-row sites between two “down” silicon atoms. This observed site-selectivity is likely due to dative bonding from the Br-atom in physisorbed 1-bromoalkanes to the partially positively charged “down” Si-atoms. Similar dative interactions were postulated for other polar molecules, such as  $\text{NH}_3$ ,<sup>42</sup>  $\text{N}(\text{CH}_3)_3$ ,<sup>43,44</sup>  $\text{CH}_3\text{Cl}$ ,<sup>3</sup> and  $\text{CH}_3\text{Br}$ <sup>4</sup> physisorbed on the same Si(100)- $c(4 \times 2)$  surface.

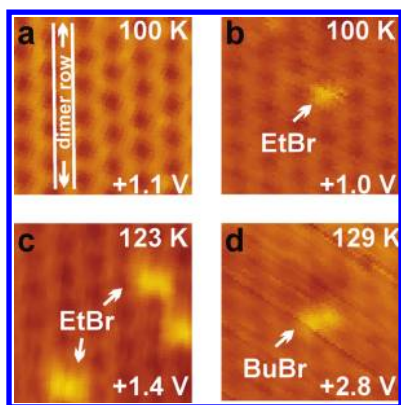


**Figure 1.** Physisorption of 1-bromoalkanes on Si(100)-c(4×2). Panel a is an empty-state image of a clean Si(100)-c(4×2) surface taken at 100 K. At imaging conditions used, only the “down” Si atoms are visible. Panels b, c, and d are typical empty-state STM images, showing the physisorption of bromoethane (EtBr) at 100 K, 1-bromopropane (PrBr) at 123 K, and 1-bromobutane (BuBr) at 129 K, respectively. All physisorbed bromoalkanes adopt the inter-row sites exclusively. All STM images are of  $\sim 38 \times 38 \text{ Å}^2$  in size, taken at the following conditions: (a)  $V_{\text{sample}} = +1.1 \text{ V}$ ,  $I = 0.2 \text{ nA}$ ; (b)  $V_{\text{sample}} = +1.0 \text{ V}$ ,  $I = 0.1 \text{ nA}$ ; (c)  $V_{\text{sample}} = +1.4 \text{ V}$ ,  $I = 0.2 \text{ nA}$ ; (d)  $V_{\text{sample}} = 2.8 \text{ V}$ ,  $I = 0.2 \text{ nA}$ .

We confirmed the assignment of the bright features as physisorbed 1-bromoalkanes, by their thermal reaction. Thermal reaction resulted in chemisorbed atomic bromine see section 3.1.3. For EtBr, we further confirmed the assignment by electron-induced reaction using a voltage pulse of +2.5 V (surface bias) for 100 ms. The observation of physisorbed EtBr on Si(100) at 100 K is, moreover, in agreement with a previous study<sup>45</sup> of the same system by ultraviolet photoelectron spectroscopy (UPS). In that study, Keeling et al. concluded that EtBr physisorbed at 110 K, as they were able to resolve the molecular  $\sigma(\text{C}-\text{Br})$  state at 4.8 eV in their UPS spectra of a dosed surface.

**3.1.2. Chemisorption; Dissociative Attachment.** Thermal DA reactions were studied by elevating the surface temperatures into the range 100–150 K. Figure 2 shows an exemplar for reaction of each physisorbed 1-bromoalkane molecule; the left-hand column shows the initial physisorbed states while the right-hand column shows the corresponding reaction products. In each case the products consisted of two fragments, one imaging bright and one imaging dark in comparison to “down” silicon atoms. The reaction products were chemisorbed at the same inter-row site as the prior physisorption site, as schematically represented in Figure 2d,d'. This close correspondence in location at the surface between reactants and products is a further example of “localized atomic reaction (LAR)”<sup>13,46,47</sup> that involves a concerted bond cleavage and formation. There is evidence<sup>8</sup> that such a concerted process leads to a significant lowering of reaction barrier, accounting for the prevailing observation of LAR on semiconductor surfaces<sup>7,8</sup> and sometimes on metals.<sup>48,49</sup>

In no case did we observe an isolated fragment as the reaction product. This absence of “abstraction” of a single bromine or alkyl-group from the physisorbed 1-bromoalkane molecules by Si(100)-c(4×2) is consistent with earlier studies from this laboratory of  $\text{CH}_3\text{Cl}^3$  and  $\text{CH}_3\text{Br}^4$  on the same surface. In contrast, abstraction was found to be the predominant dissociation mechanism for haloalkanes<sup>46,50–54</sup> on Si(111)-(7×7). On Si(111)-(7×7), adatoms are 6.7 or 7.7 Å apart, whereas adjacent Si adatoms at inter-row sites of Si(100)

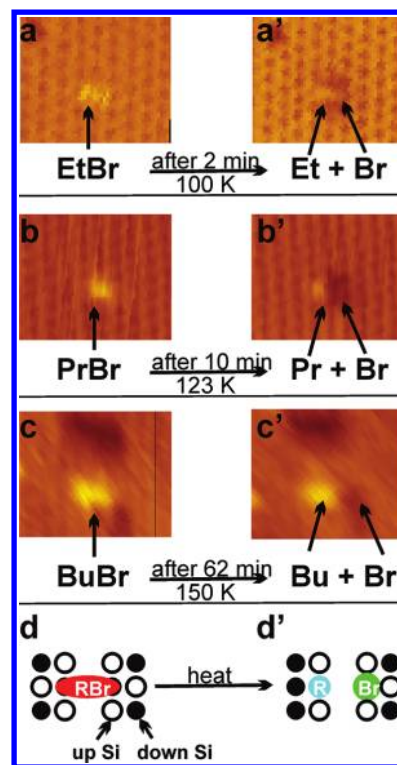


**Figure 2.** Thermal dissociation events imaged for (a,a') bromoethane at 100 K, (b,b') 1-bromopropane at 123 K, (c,c') 1-bromobutane at 150 K, with schematics given in panel d,d'. All STM images ( $\sim 64 \times 54 \text{ Å}^2$  in size) were taken at the following conditions: (a and a')  $V_{\text{sample}} = +1.1 \text{ V}$ ,  $I = 0.2 \text{ nA}$ ; (b and b')  $V_{\text{sample}} = +1.4 \text{ V}$ ,  $I = 0.2 \text{ nA}$ ; (c and c')  $V_{\text{sample}} = +1.0 \text{ V}$ ,  $I = 0.05 \text{ nA}$ . In all panels, dimer rows run vertically.

are separated by only 5.2 Å and hence may participate more readily in a concerted bond cleavage plus formation process that leads to the exclusively observed DA outcome. Similar correlation between adatom separation and dissociation dynamics was proposed by Rezaei, Stipe, and Ho to account for their observed contrasting dissociation behaviors of chemisorbed DS (from  $\text{D}_2\text{S}$ ) on Si(100)<sup>55</sup> and Si(111)<sup>56</sup> surfaces.

The reaction products of DA of the three 1-bromoalkanes considered here are atomic bromine and its corresponding alkyl group, both chemisorbed onto the surface. The products of DA are clearly chemisorbed, as they exhibit far greater thermal stabilities than the physisorbed 1-bromoalkanes. Upon heating the dosed surfaces (as in Figure 2a–c) individually to 180 K, we observed DA products to complete exclusion of physisorbed 1-bromoalkanes, for all three cases. The observed relative thermal stabilities of physisorbed and chemisorbed species are also consistent with the previous UPS study<sup>45</sup> of EtBr on the same Si(100) surface. We assign the fragments that image brighter than “down” Si-atoms as chemisorbed alkyl groups, and the fragments that image darker than “down” Si-atoms as chemisorbed bromine atoms, as shown in the right column of Figure 2. Our assignment is based on comparison of the buckling direction of the reacted Si-dimers between our STM images and ab initio calculations. See Supporting Information for details.

**3.1.3. Activation Energies,  $E_a$ 's, for Dissociative Attachment.** The barriers to thermal reaction for EtBr, PrBr, and BuBr were measured experimentally by observing populations of physisorbed molecules react. In each measurement, a surface



area was imaged for a sufficient length of time for a statistically useful sample of molecules to dissociate. The reactions were followed at 100 K for EtBr, at 123 K for PrBr, and at 150 K for BuBr. Possible tip-induced effects<sup>57</sup> were carefully considered and found to have a negligible effect on reaction rates. (See Supporting Information for details.)

As shown in Figure 3, the thermal reaction rates were determined using first order kinetics by fitting the fractional

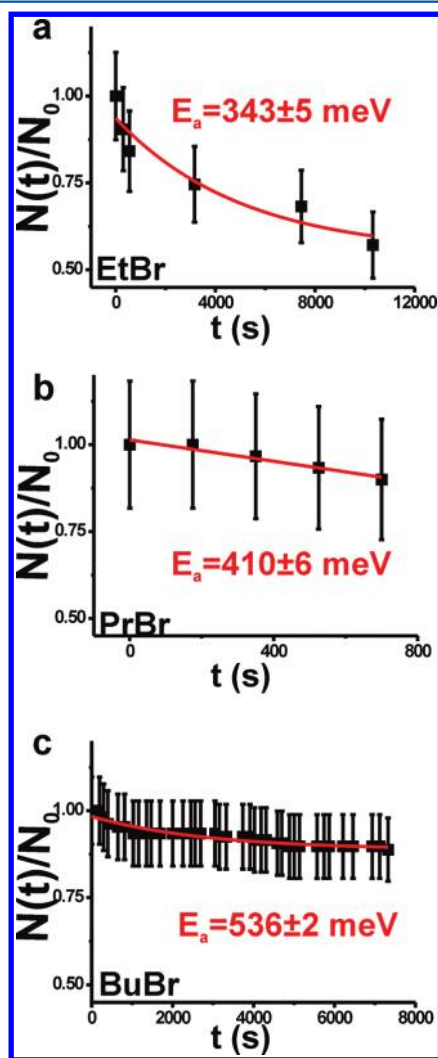


**Figure 3.** Graphs of the fractional survival of unreacted physisorbed molecule against time for EtBr at 100 K (in panel a), PrBr at 123 K (in panel b), and BuBr at 150 K (in panel c), on Si(100)-c(4×2). By fitting the experimental measurements to first order exponential decay formula (red curve in each panel), we were able to calculate the thermal activation energies, as  $E_a = 343 \pm 5$  meV for EtBr,  $E_a = 410 \pm 6$  meV for PrBr, and  $E_a = 536 \pm 2$  meV for BuBr, assuming an Arrhenius formula with a prefactor of  $10^{13} \text{ s}^{-1}$ . The experimental uncertainties are statistical, taken as the square-root of the counts, rather than from misidentifying reactive events.

survival of physisorbed molecules,  $N(t)/N_0$ , against time ( $t$ ) to exponential decay,  $N(t)/N_0 = \exp(-kt)$ . In this fit,  $N_0$  is the initial count of physisorbed 1-bromoalkanes at the start of each measurement, and  $k$  is the decay (rate) constant. We obtained decay constants individually, as  $k_1 = (5.0 \pm 0.3) \times 10^{-5} \text{ s}^{-1}$  for EtBr,  $k_2 = (1.6 \pm 0.7) \times 10^{-4} \text{ s}^{-1}$  for PrBr, and  $k_3 = (1.0 \pm 0.1) \times 10^{-5} \text{ s}^{-1}$  for BuBr.

We derived the activation energies for the thermal DA reactions of all three 1-bromoalkanes by assuming an Arrhenius formula and a common prefactor of  $10^{13} \text{ s}^{-1}$ .<sup>15,46,58</sup> We find  $E_a = 343 \pm 5$  meV for EtBr,  $E_a = 410 \pm 6$  meV for PrBr, and  $E_a = 536 \pm 2$  meV for BuBr. The uncertainties given are relative uncertainties arising from the uncertainties in the fitted decay constants. The absolute uncertainty, which is to be applied to all three measurements simultaneously is far greater. The assumed prefactor of  $10^{13} \text{ s}^{-1}$  neglects entropic effects and is the greatest source of uncertainty; we estimate the absolute uncertainty as 50 meV, using a wider range of  $10^{13 \pm 2} \text{ s}^{-1}$  for the prefactor.<sup>59,60</sup> However, in present case, it is relative energies that are of interest, and the systems being compared are all 1-bromoalkane on Si(100)-c(4×2); assuming the same prefactor in all cases should be an excellent approximation.

During our thermal rate measurements we observed no other processes accompanying the reactions, such as molecular migration or desorption. This observation enables us to conclude, for all three cases, that physisorption energies are significantly higher than reaction barriers to DA. Further, the measured reaction barriers to DA may also be regarded as lower limits for the corresponding physisorption energies. This is of interest when considering appropriate theoretical methods; see Supporting Information.

**3.2. Theory. 3.2.1. DFT versus DFT-D.** Both standard DFT and also DFT-D methods,<sup>14</sup> that include some allowance for dispersion forces, were employed to investigate physisorption and reaction of 1-bromoalkanes on Si(100)-c(4×2). The geometries obtained by both methods were similar, but the corresponding energies were greatly different. The limitation of standard DFT methods mainly arises from underestimated physisorption energies, as also found in earlier work<sup>59,60</sup> from this laboratory. This is because standard DFT does not properly account for van der Waals interactions (dispersion interaction) that are important in physisorption. The DFT-D method<sup>14</sup> was developed to overcome these limitations and gives better agreement with the experimentally derived physisorption and activation energies. In the following, only results from DFT-D calculations are presented. Refer to Supporting Information for calculation details.

**3.2.2. Physisorption.** The most stable geometries from our DFT-D computations for physisorbed 1-bromoalkanes are represented in Figure 4a–c. For clarity, the full supercell is not shown; only the adsorbate and the 12 Si-atoms underneath are given. The choice of the initial configuration was guided by experiment: we therefore considered only inter-row adsorption geometries between two “down” Si-atoms.

For all three cases, the most stable physisorbed geometries<sup>61</sup> calculated by DFT-D were aligned horizontally with the Br atom almost above one “down” Si-atom, with a short Br...Si separation of  $\sim 2.5$  Å. This close separation is only 0.3 Å longer than the covalent Br–Si bond length of 2.29 Å,<sup>62</sup> in line with our anticipated dative bonding between the lone pair bromine electrons and positively charged down Si-atom. Despite the close approach of the Br atom toward the Si down atom, we consider these states as physisorbed 1-bromoalkanes because the C–Br separations ( $\sim 2.0$  Å) were essentially unchanged from those in the free molecules (1.93 Å).<sup>62</sup> Similar horizontal molecular adsorption geometries for 1-haloalkanes were also reported on copper surfaces.<sup>15</sup>

The calculated adsorption energies determined by DFT-D for these three 1-bromoalkanes were  $E_{\text{ads}} = 853$  meV for EtBr,  $E_{\text{ads}} = 914$  meV for PrBr, and  $E_{\text{ads}} = 970$  meV for BuBr,

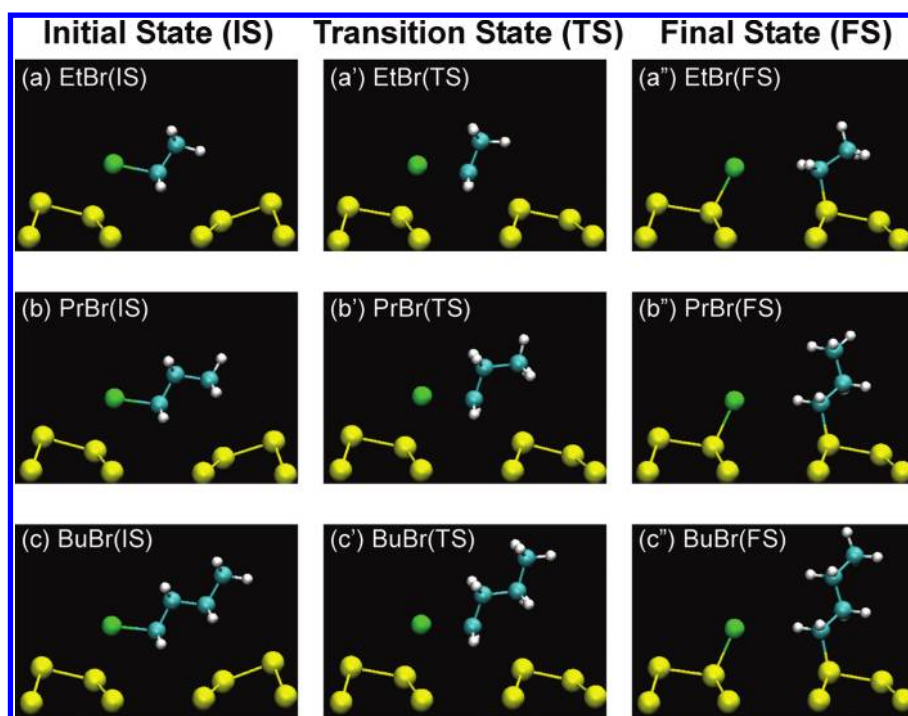


**Figure 4.** Physisorption and dissociative attachment (DA) of EtBr, PrBr, and BuBr computed by DFT-D. Initial physisorbed configurations (left column) and final chemisorbed configurations (right column) were separately optimized. Transition states (middle column) were calculated using the climbing image nudged elastic band (CI-NEB) technique.

consistent with the nature of physisorption. The physisorption energies increase with alkyl chain-length, the increase being  $\sim 50$  meV per  $\text{CH}_2$  group, consistent with previous studies that all found a similar increase of 50–100 meV per additional  $\text{CH}_2$  group in measured heats of adsorption, for 1-bromoalkanes on Cu(111),<sup>15</sup> 1-bromoalkanes on GaAs(110),<sup>63</sup> alkanes on Cu(111),<sup>64</sup> alkanes on Pt(111),<sup>64</sup> alkanes on  $\text{TiO}_2(110)$ ,<sup>65</sup> 1-alcohols on Ag(110),<sup>66</sup> and 1-alcohols on  $\text{TiO}_2(110)$ .<sup>67</sup> Such increases in heats of adsorption are usually interpreted as an increased van der Waals interaction between the extra  $\text{CH}_2$  group with the surface.

**3.2.2. Chemisorption by Dissociative Attachment.** The geometries of the chemisorbed reaction products at their inter-row sites were optimized in a manner similar to that used for physisorbed molecules. The most stable configurations for the reaction products of EtBr, PrBr, and BuBr are shown in Figure 4a'',b'',c'', respectively. In these configurations, the alkyl groups are all directed away from the surface in an "upright" (vertical) geometry. It might be thought that further energy would be gained by bringing the alkyl chain closer to the silicon surface, but this results in less stable geometries. Similar "upright" geometries for chemisorbed alkyl chains have also been reported on copper<sup>15</sup> and aluminum<sup>68</sup> surfaces. In the chemisorbed configurations for the DA products of all three 1-bromoalkanes, the Si-dimer to which alkyls attach reverses the buckling directions from each of the corresponding initial physisorption configuration, but the buckling direction for the brominated Si-dimer was preserved. This subtle signature enables us to assign the reaction products from DA, see Supporting Information.

The products of DA reactions are chemisorbed, with binding energies calculated by DFT-D as  $D = 2.802$  eV for EtBr,  $D = 2.856$  eV for PrBr and  $D = 2.874$  eV for BuBr. The calculated bond lengths are also consistent with chemisorption; the Br–Si

separations being  $\sim 2.3$  Å, while the C–Si separation is  $\sim 1.9$  Å, close to the literature values of covalent bond lengths of 2.21 Å for Br–Si and 1.87 Å for C–Si.<sup>62</sup>

**3.2.3. Transition States Determined by CI-NEB.** The energy barriers to reaction were obtained using the CI-NEB method as implemented in VASP. The transition state geometries were obtained using both DFT/CI-NEB and DFT-D/CI-NEB methods. Both methods gave similar results, but it is the DFT-D derived geometries that are given in Figure 4a',b',c', respectively, for the DA reactions of EtBr, PrBr, and BuBr on Si(100)-c(4x2). In the transition state geometries of all three 1-bromoalkanes, the Si-dimer under the alkyl chain has changed its buckling direction close to the geometry of the final state, lifting the "down" Si-atom toward the alkyl group.<sup>69</sup> Also in the transition states the alkyl chains are substantially displaced from their initial physisorption states, being situated midway between the Br-atom (to which it was bound) and Si-atom (to which it will be bound). The C–Br bond length extends from  $\sim 2.0$  Å (in IS, initial state) to  $\sim 2.3$  Å (in TS, transition state), and concurrently the C–Si distance decreases from  $\sim 3.5$  to  $3.7$  Å (in IS) to  $\sim 2.8$  to  $2.9$  Å (in TS), which is part way to the length of 1.87 Å for C–Si covalent bond. This compact transition state is suggestive of the coexistence of the old and new bonds in concerted reaction, consistent with the observed LAR.

The activation energies for DA were computed by DFT-D/CI-NEB as  $E_c = 317$  meV for EtBr,  $E_c = 406$  meV for PrBr, and  $E_c = 430$  meV for BuBr, in good agreement with the experimental values of  $E_a = 343 \pm 5$  meV for EtBr,  $E_a = 410 \pm 6$  meV for PrBr, but not for BuBr, which has an experimentally determined  $E_a$  of  $536 \pm 2$  meV. The computed activation energies for all are significantly lower than the corresponding computed physisorption energies, consistent with our experimental observations of dissociation to the total

exclusion of desorption during extensive thermal-rate measurements.

## 4. DISCUSSION

**4.1. Interpretation of Increased Thermal Barrier with Chain-Length.** Strikingly, we found experimentally that the thermal barrier to DA increases with chain-length, by  $\sim 100$  meV per  $\text{CH}_2$  unit, for EtBr, PrBr, and BuBr on  $\text{Si}(100)\text{-c}(4\times 2)$ . This trend is also consistent with the upper limit for the thermal barrier of  $E_a < \sim 200$  meV for the further example of  $\text{CH}_3\text{Br}$  on the same surface.<sup>70</sup> The trend found here is in a sharp contrast to the dissociation in the gas-phase where no variation with chain-length was reported for C–Br dissociation energies, within experimental uncertainties. The experimental and calculated thermal barriers for the dissociation on  $\text{Si}(100)\text{-c}(4\times 2)$  are summarized in Table 1, in comparison with the documented gas phase dissociation energies of C–Br bonds,  $D_e(\text{C–Br, gas})$ .<sup>71</sup>

**Table 1. Comparison of Energies**

molecule	$E_a$ in meV (experiment)	$E_c$ in meV (DFT-D)	$D_e(\text{C–Br, gas})$ in eV <sup>71</sup>
EtBr	$343 \pm 5$	317	$3.04 \pm 0.04$
PrBr	$410 \pm 6$	406	$3.09 \pm 0.04$
BuBr	$536 \pm 2$	430	$3.07 \pm 0.04$

The observed increase in activation energy for DA along the series of 1-bromoalkanes (EtBr, PrBr, and BuBr) is reproduced in our DFT-D calculations. The geometries of the four-atom reactive center, Si–Br–C–Si, are essentially identical for all three 1-bromoalkanes, for both initial physisorbed states and transition states. Since the major variable is the alkyl chain-length, the observed increase in energy required in order to reach the TS would appear to arise from energy required to reconfigure, i.e., specifically to raise, the extra  $(\text{CH}_2)_2$  segments in successively longer chains.

As discussed and as evident in Figure 5, the principal difference between the initial physisorbed states and the transition states is the lifting of the alkyl chain away from the surface. This movement is accompanied by a flip of the silicon-dimer beneath the alkyl tail.<sup>69</sup> This is shown in Figure 5, where we overlay the initial states and transition states for all three cases in Figure 5a,b,c; the lifting is shown to be 0.6–0.7 Å. In going from initial state to transition state, the terminal carbon atoms in the physisorbed PrBr and the penultimate and terminal carbon atoms in the physisorbed BuBr are lifted away from the surface by 0.6, 0.6, and 0.7 Å, respectively. There is no corresponding displacement in the case of EtBr. The energy cost of flipping the Si-dimer was found to be independent of the physisorbed 1-bromoalkanes. Accordingly, we attribute this increased activation energy with increase in chain-length to the energy required to lift the alkyl chain away from the surface as the length of the alkyl chain increases. For dissociation in the gas phase, the absence of the underlying surface leads to dissociation energies independent of alkyl chain-length.

In a relevant earlier study,<sup>15</sup> Lin and Bent found no dependence of thermal dissociation rates with alkyl chain-length for a series of 1-bromoalkanes on  $\text{Cu}(111)$ . Their high-resolution energy loss spectroscopy (HREELS) data suggested, as is the case here, a horizontal alignment of the alkyl chains in physisorbed 1-bromoalkanes geometry (IS) and a vertical alignment of alkyl chains in chemisorbed alkyl geometry (FS).

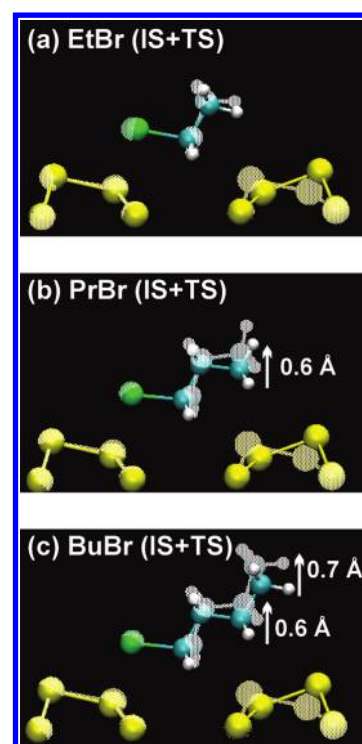


**Figure 5.** Overlaid computed geometries for 1-bromoalkanes: (a) EtBr, (b) PrBr, and (c) BuBr on  $\text{Si}(100)\text{-c}(4\times 2)$ . In each panel, initial state (IS) and transition state (TS) geometries are represented in solid and shadowed colors, respectively, with the arrows indicating the change in geometry of the alkyl chain from IS to TS.

They speculated that the lifting of the alkyl chain occurred subsequent to transition state (TS). This is in contrast to our current study on  $\text{Si}(100)\text{-c}(4\times 2)$ , in which the dissociation barrier increases experimentally with the alkyl chain-length, and extensive calculation shows that the lifting of the alkyl chain occurs prior to the transition state.

**4.2. Inter-Row Dissociative Attachment and Si-Dimer Flipping.** A noteworthy feature of the present study is the observation of inter-row DA to the total exclusion of inter-dimer DA and on-dimer DA. This observation is in qualitative accord with an earlier study<sup>4</sup> of this laboratory of the dissociation of  $\text{CH}_3\text{Br}$  on a  $\text{Si}(100)\text{-}2 \times 1$  surface, performed at 270 K. In that work, it was found that the inter-row DA was the predominant pathway (88%), but significant DA was also observed to occur to inter-dimer sites (11%), and on-dimer sites (1%).

The earlier study of  $\text{CH}_3\text{Br}$  was carried out at 270 K,<sup>4</sup> and at that temperature the rate of Si-dimer flipping is comparable to the molecular adsorption rate from background exposure ( $10^{-8}$  to  $10^{-10}$  Torr).<sup>72</sup> The Si-dimer flipping enables the possibility of a transient state of the silicon surface in which two adjacent Si-atoms are “down” at both the inter-dimer or on-dimer sites.<sup>73</sup> Such dimer flipping motions were slow at the temperature range 50–180 K in the present study, giving the  $\text{c}(4\times 2)$  reconstruction that only permits two adjacent “down” Si atoms at the inter-row site. The alteration in surface mobility between the two different measurement temperatures may account for the exclusively inter-row DA found here for longer 1-bromoalkanes at a reduced surface temperature (50–180 K) as compared with the multiple dissociation pathways observed for  $\text{CH}_3\text{Br}$  at the higher temperature (270 K). A similar correlation between surface temperature and DA outcome has



also been found from this laboratory for 1,2-dichloroethane and 1,2-dibromoethane on Si(100) surface.<sup>74,75</sup> Such a flipping motion of Si dimers was also recently proposed to account for the dissociation dynamics of  $\text{NH}_3$ <sup>6</sup> and  $\text{H}_2\text{O}$ <sup>72</sup> on Si(100).

**4.3. Proposed Effect of “Dynamical Delay”.** For EtBr and PrBr, experiment ( $E_a = 343 \pm 5$  meV for EtBr, and  $E_a = 410 \pm 6$  meV for PrBr) and theory ( $E_c = 317$  meV for EtBr and  $E_c = 406$  meV for PrBr) are in good accord regarding the activation energies. The percentage of deviation from theory,  $(E_a - E_c)/E_a$ , is only  $\sim 8\%$  for EtBr and  $\sim 1\%$  for PrBr. This was expected in view of the tests that were made of the accuracy of the calculation for the initial, final, and transition states, as noted in the Methods section (tests included zero-point energies). The calculated physisorption energies increased monotonically with chain-length up to and including BuBr, as expected from previous studies.<sup>15,63–67</sup> We believe it to be significant, therefore, that the barrier height calculated for the case of BuBr ( $E_c = 430$  meV) deviated from experimental value ( $E_a = 536 \pm 2$  meV) by 20%. We suggest, below, that this large discrepancy between experiment and theory for BuBr may be due to a dynamical effect.

The computed transition state geometries for all the three 1-bromoalkanes require that the C–Br bond is stretched with a synchronous lift of the alkyl chain.<sup>69</sup> It appears possible that a “delay” in the lifting motion of the alkyl chain might occur for the longest of the 1-bromoalkanes studied, BuBr. Hence, in the reaction of BuBr on Si(100)-c(4×2), the long alkyl chain might prevent the system from achieving the optimal configuration for barrier-crossing in the transit time between the initial state and the transition state (Figure 4c'). Such a “dynamical delay” would cause the average trajectory to cross the barrier at a higher energy than the minimum that was calculated.

To examine the proposed mechanism of “dynamical delay”, we calculated the energy increase that would occur if the transition state geometry were distorted by bending the 1-propyl group at the  $\alpha$ -carbon atom downward to the underlying surface. As shown in Figure 6a,b, a distortion angle of only  $\sim 8^\circ$  would account for the discrepancy of 106 meV between experiment and theory.

Vibration-to-vibration energy-transfer from an anharmonic C–H bond along a harmonically coupled carbon-chain is calculated to have a characteristic relaxation time of  $\sim 100$  fs (independent of chain-length).<sup>76</sup> In the present case, the reactive stretching of the terminal C–Br bond must be converted into bending of the alkyl-tail, which, due to frequency-mismatch between stretch and bend, would be expected to have a relaxation time  $> 100$  fs. It appears plausible, therefore, that during the short transition time between the initial state and the transition state there could be a “lag” in bending. The answer is to be found in a statistical group of trajectories.<sup>20,77</sup> This is, however, beyond the scope of present study. It will be interesting to look for this effect in other studies of the reaction dynamics of molecular adsorbates possessing long alkyl chains.

## 5. CONCLUSIONS

We have used STM to study the physisorption and subsequent DA of EtBr, PrBr, and BuBr on Si(100)-c(4×2). In all three cases, molecular 1-bromoalkanes physisorbed exclusively over the inter-row site of Si(100)-c(4×2) between two adjacent topographically depressed “down” Si adatoms. Localized DA reaction was induced by heat, and activation energies for thermal reaction were measured as  $E_a = 343 \pm 5$  meV for EtBr,  $E_a = 410 \pm 6$  meV for PrBr, and  $E_a = 536 \pm 2$  meV for BuBr. These experiments reveal for the first time that the barrier to

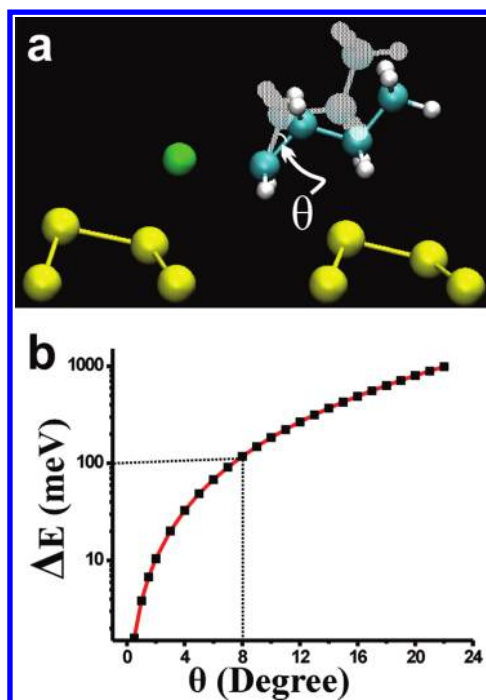


**Figure 6.** (a) Shadowed alkyl chain for BuBr is shown in its computed TS configuration, whereas the colored representation shows the effect of a delay in lifting the chain resulting in a deviation by an angle  $\theta$  from the TS configuration measured from C(1) to C(2). (b) Computed energy-change with increasing deviation,  $\theta$ , from the TS. The observed increase in experimentally measured  $E_a$  relative to computed  $E_c$  ( $\Delta E = 106$  meV) would require a “dynamical lag” of  $\theta = 8^\circ$ .

thermal DA increases with chain-length, by  $\sim 100$  meV per  $\text{CH}_2$  unit. This systematic increase in barrier height is in partial agreement with our ab initio DFT-D calculations that yield a computed barrier of  $E_c = 317$  meV for EtBr,  $E_c = 406$  meV for PrBr, and  $E_c = 430$  meV for BuBr. We interpret this trend of increasing thermal barriers as being due to the additional energy required to lift the longer alkyl-group away the surface in going from the initial physisorbed state to the reactive transition state. The substantially greater discrepancy between theory and experiment for BuBr, it is suggested, is speculated to be due to a “dynamical lag” in lifting the alkyl chain.

## ■ ASSOCIATED CONTENT

### Supporting Information

STM imaging behaviors of physisorbed 1-bromoalkane on Si(100)-c(4×2), product fragment assignment, evidence of negligible tip-induced effect in measuring barrier height, DFT and DFT-D calculation details, quantum zero-point energy effect on computed barrier height, and complete author lists for refs 32 and 52. This material is available free of charge via the Internet at <http://pubs.acs.org>.

## ■ AUTHOR INFORMATION

### Corresponding Author

\*E-mail: [jpolanyi@chem.utoronto.ca](mailto:jpolanyi@chem.utoronto.ca).

### Present Addresses

<sup>†</sup>Department of Chemistry, University of California, Riverside, 501 Bing Springs Road, Chemical Sciences #139, Riverside, California 92521, United States.

<sup>‡</sup>School of Biological Sciences and Applied Chemistry, Seneca College, 70 The Pond Road, Toronto, Ontario M3J 3M6, Canada.



## Notes

The authors declare no competing financial interest.

## ■ ACKNOWLEDGMENTS

We are grateful for financial support from the Natural Sciences and Engineering Research Council of Canada (NSERC), the Xerox Research Centre Canada (XRCC), and the Canadian Institute for Advanced Research (CIFAR). We thank Prof. Wei Ji at Renmin University of China for helpful discussions. S.Y.G. is supported by the Fonds Québécois de la Recherche sur la Nature et les Technologies (FQRNT). M.S. was supported for this work by an Undergraduate Student Research Award (USRA) from NSERC. Computations were performed on the Tightly Coupled System (TCS) supercomputer at the SciNet HPC Consortium. SciNet is funded by the Canada Foundation for Innovation under the auspices of Compute Canada, the Government of Ontario, Ontario Research Fund—Research Excellence, and the University of Toronto.

## ■ REFERENCES

- (1) Gasser, R. P. H. *An Introduction to Chemisorption and Catalysis by Metals*; Oxford University Press: Oxford, U.K.; 1985, p 5.
- (2) De Pisto, A. E. In *Dynamics of Gas-Surface Interactions*; Rettner, C. T., Ashfold, M. N. R., Eds.; The Royal Society of Chemistry: London, 1991, p 47.
- (3) Lim, T.; Polanyi, J. C.; Guo, H.; Ji, W. *Nat. Chem.* **2011**, *3*, 85 and its Supplementary Information.
- (4) Lim, T. B.; McNab, I. R.; Polanyi, J. C.; Guo, H.; Ji, W. *J. Am. Chem. Soc.* **2011**, *133*, 11534 and its Supporting Information.
- (5) Bent, B. E. *Chem. Rev.* **1996**, *96*, 1361 and references therein.
- (6) Owen, J. H. G. *J. Phys.: Condens. Matter* **2009**, *21*, 443001 and references therein.
- (7) McNab, I. R.; Polanyi, J. C. *Chem. Rev.* **2006**, *106*, 4321 and references therein.
- (8) McNab, I. R.; Polanyi, J. C. Chapter 4: Imprinting Atomic and Molecular Patterns. In *Atomic and Molecular Manipulation*; Mayne, A. J., Dujardin, G., Eds.; Elsevier Ltd.: New York, 2011, pp 79 and references therein, <http://www.sciencedirect.com/science/article/pii/B9780080963556000040>.
- (9) Leftwich, T. R.; Teplyakov, A. V. *Surf. Sci. Rep.* **2008**, *63*, 1 and references therein.
- (10) Laerdahl, J. K.; Uggerud, E. *Int. J. Mass Spectrom.* **2004**, *214*, 277 and references therein.
- (11) McMurry, J. *Organic Chemistry*, 6th ed.; Thomson Learning, Inc., 2004; pp 350–351.
- (12) Smyth, C. *J. Am. Chem. Soc.* **1941**, *63*, 57.
- (13) Lu, P. H.; Polanyi, J. C.; Rogers, D. J. *Chem. Phys.* **1999**, *111*, 9905.
- (14) Grimme, S. *J. Comput. Chem.* **2006**, *27*, 1787.
- (15) Lin, J.-L.; Bent, B. E. *J. Phys. Chem.* **1992**, *96*, 8529.
- (16) Kuntz, P. J.; Nemeth, E. M.; Polanyi, J. C. *J. Phys. Chem.* **1969**, *50*, 4607.
- (17) Kuntz, P. J.; Nemeth, E. M.; Polanyi, J. C. *J. Phys. Chem.* **1969**, *50*, 4623.
- (18) Nazar, M. A.; Polanyi, J. C.; Skrlac, W. J. *Chem. Phys. Lett.* **1974**, *29*, 473.
- (19) Yan, S.; Wu, Y.-T.; Zhang, B.; Yue, X. F.; Liu, K. *Science* **2007**, *316*, 1723.
- (20) Yan, S.; Wu, Y.-T.; Liu, K. *Proc. Natl. Acad. Sci. U.S.A.* **2008**, *105*, 12667.
- (21) Shepler, B. C.; Braams, B. J.; Bowman, J. M. *J. Phys. Chem. A* **2008**, *112*, 9344.
- (22) Suits, A. G. *Acc. Chem. Res.* **2008**, *41*, 873 and references therein.
- (23) Czako, G.; Bowman, J. M. *Science* **2011**, *334*, 343.
- (24) Smith, R. R.; Killelea, D. R.; DelSesto, D. F.; Utz, A. L. *Science* **2004**, *304*, 992.
- (25) Maroni, P.; Papageorgopoulos, D. C.; Sacchi, M.; Dang, T. T.; Beck, R. D.; Rizzo, T. R. *Phys. Rev. Lett.* **2005**, *94*, 246104.
- (26) Yoder, L. B.; Bisson, R.; Beck, R. D. *Science* **2010**, *329*, 553.
- (27) Yoder, L. B.; Bisson, R.; Hundt, P. M.; Beck, R. D. *J. Chem. Phys.* **2011**, *135*, 224703.
- (28) Hata, K.; Kimura, T.; Ozawa, S.; Shigekawa, H. *J. Vac. Sci. Technol., A* **2000**, *18*, 1933.
- (29) Hossain, M. Z.; Yamashita, Y.; Mukai, K.; Yoshinobu, J. *Phys. Rev. B* **2003**, *67*, 153307.
- (30) Kresse, G.; Hafner, J. *Phys. Rev. B* **1993**, *47*, 558.
- (31) Kresse, G.; Furthmüller, J. *Phys. Rev. B* **1996**, *54*, 11169.
- (32) Loken, C.; Gruner, D.; Groer, L.; Peltier, R.; Bunn, N.; Craig, M.; Henriques, T.; Dempsey, J.; Yu, C.-H.; Chen, J.; et al. *J. Phys.: Conf. Ser.* **2010**, *256*, 012026.
- (33) Perdew, J. P.; Ernzerhof, M.; Burke, K. *J. Chem. Phys.* **1996**, *105*, 9982.
- (34) Blochl, P. E. *Phys. Rev. B* **1994**, *50*, 17953.
- (35) Kresse, G.; Joubert, D. *Phys. Rev. B* **1999**, *59*, 1758.
- (36) Henkelman, G.; Uberuaga, B. P.; Jonsson, H. *J. Chem. Phys.* **2000**, *113*, 9901.
- (37) Humphrey, W.; Dalke, A.; Schulten, K. *J. Mol. Graphics* **1996**, *14*, 33.
- (38) Henkelman, G.; Arnaldsson, A.; Jonsson, H. *J. Chem. Phys.* **2006**, *124*, 044706.
- (39) Wolkow, R. A. *Phys. Rev. Lett.* **1992**, *68*, 2636.
- (40) Chadi, D. J. *Phys. Rev. Lett.* **1979**, *43*, 43.
- (41) Hata, K.; Yasuda, S.; Shigekawa, H. *Phys. Rev. B* **1999**, *60*, 8164.
- (42) Hossain, M. Z.; Yamashita, Y.; Mukai, K.; Yoshinobu, J. *Phys. Rev. B* **2003**, *68*, 235322.
- (43) Hossain, M. Z.; Machida, S.-I.; Yamashita, Y.; Mukai, K.; Yoshinobu, J. *J. Am. Chem. Soc.* **2003**, *125*, 9252.
- (44) Hossain, M. Z.; Machida, S.-I.; Nagao, M.; Yamashita, Y.; Mukai, K.; Yoshinobu, J. *J. Phys. Chem. B* **2004**, *108*, 4737.
- (45) Keeling, L. A.; Chen, L.; Greenlief, C. M.; Mahajan, A.; Bonser, D. *Chem. Phys. Lett.* **1993**, *217*, 136.
- (46) Guo, H.; Ji, W.; Polanyi, J. C.; Yang, J. (S. Y.). *ACS Nano* **2008**, *2*, 699.
- (47) Harikumar, K. R.; McNab, I. R.; Polanyi, J. C.; Zabet-Khosousi, A.; Hofer, W. A. *Proc. Natl. Acad. Sci. U.S.A.* **2011**, *108*, 950.
- (48) Maksymovych, P.; Yates, J. T., Jr. *J. Am. Chem. Soc.* **2006**, *128*, 10642.
- (49) Leung, L.; Lim, T.; Polanyi, J. C.; Hofer, W. A. *Nano Lett.* **2011**, *11*, 4113.
- (50) Dobrin, S.; Harikumar, K. R.; Polanyi, J. C. *J. Phys. Chem. B* **2006**, *110*, 8010.
- (51) Dobrin, S.; Harikumar, K. R.; Jones, R. V.; McNab, I. R.; Polanyi, J. C.; Waqar, Z.; Yang, J. (S. Y.). *J. Chem. Phys.* **2006**, *125*, 133407.
- (52) Dobrin, S.; Harikumar, K. R.; Lim, T. B.; Leung, L.; McNab, I. R.; Polanyi, J. C.; Sloan, P. A.; Waqar, Z.; Yang, J. (S. Y.); Ayissi, S.; et al. *Nanotechnology* **2007**, *18*, 044012.
- (53) Ebrahimi, M.; Huang, K.; Lu, X.; McNab, I. R.; Polanyi, J. C.; Waqar, Z.; Yang, J. (S. Y.); Lin, H.; Hofer, W. A. *J. Am. Chem. Soc.* **2011**, *133*, 16560 and its Supporting Information.
- (54) Eisenstein, A.; Harikumar, K. R.; Huang, K.; McNab, I. R.; Polanyi, J. C.; Zabet-Khosousi, A. *Chem. Phys. Lett.* **2012**, *527*, 1.
- (55) Rezaei, M. A.; Stipe, B. C.; Ho, W. J. *Chem. Phys.* **1998**, *110*, 3548.
- (56) Rezaei, M. A.; Stipe, B. C.; Ho, W. J. *Chem. Phys.* **1998**, *109*, 6075.
- (57) Mayne, A.; Dujardin, G.; Comtet, G.; Riedel, D. *Chem. Rev.* **2006**, *106*, 4355.
- (58) Nagao, M.; Mukai, K.; Yamashita, Y.; Yoshinobu, J. *J. Phys. Chem. B* **2004**, *108*, 5703.
- (59) Harikumar, K. R.; Leung, L.; McNab, I. R.; Polanyi, J. C.; Lin, H.; Hofer, W. A. *Nat. Chem.* **2009**, *1*, 716 and its Supplementary Information.

(60) Harikumar, K. R.; McNab, I. R.; Polanyi, J. C.; Zabet-Khosousi, A.; Panosetti, C.; Hofer, W. A. *Chem. Commun.* **2011**, 47, 12101 and its electronic Supplementary Information.

(61) The most stable geometries were obtained by relaxing trial configurations in which the 1-bromoalkane molecules were horizontally aligned with respect to the surface. Optimizations that started from trial configurations with a vertical or tilted molecular alignment led to less stable configurations.

(62) *CRC Handbook of Chemistry and Physics*, 92nd ed.; Haynes, W. M., Lide, D. R., Eds.; CRC Press: Boca Raton, FL, 2011; pp 9–48.

(63) Khan, K. A.; Camillone, N., III; Osgood, R. M., Jr. *J. Phys. Chem. B* **1999**, 103, 5530.

(64) Lei, R. Z.; Gellman, A. J.; Koel, B. E. *Surf. Sci.* **2004**, 554, 125.

(65) Zhang, Z.; Rousseau, R.; Gong, J.; Kay, B. D.; Dohnalek, Z. *J. Am. Chem. Soc.* **2009**, 131, 17926.

(66) Zhang, R.; Gellman, A. J. *J. Phys. Chem.* **1991**, 95, 7433.

(67) Li, Z.; Smith, R. S.; Kay, B. D.; Dohnalek, Z. *J. Phys. Chem. C* **2011**, 115, 22534.

(68) Bent, B. E.; Nuzzo, R. R.; Zegarski, B. R.; Dubois, L. H. *J. Am. Chem. Soc.* **1991**, 113, 1137.

(69) Our CI-NEB calculations show that the DA reactions for 1-bromoalkanes consist of two sequential processes, each with a distinguished barrier: (a) The first barrier associates with the reverse of Si-dimer buckling direction. (b) Subsequently, the second barrier associates with stretch of C–Br bond and the lift of alkyl-chains. For all three cases, the first barrier is lower than the second barrier. Therefore, we identify the transition states in each case for the second barrier as the global transition states and report them in detail in the main text.

(70) This upper limit is estimated from a preliminary study that observed the completion of the dissociation for CH<sub>3</sub>Br within 15 min after exposure to Si(100)-c(4×2) at 50 K.

(71) Luo, Y.-R. *Comprehensive Handbook of Chemical Bond Energies*; CRC Press: Boca Raton, FL, 2007; pp 237–238.

(72) Yu, S.-Y.; Kim, Y.-S.; Kim, H.; Koo, J.-Y. *J. Phys. Chem. C* **2011**, 115, 24800.

(73) Hayes, R. L.; Tuckerman, M. E. *J. Am. Chem. Soc.* **2007**, 129, 12172.

(74) Harikumar, K. R.; Polanyi, J. C.; Zabet-Khosousi, A.; Czekala, P.; Lin, H.; Hofer, A. W. *Nat. Chem.* **2011**, 3, 400 and its Supplementary Information.

(75) Huang, K. Ph.D. Thesis, Department of Chemistry, University of Toronto, Toronto, 2011; pp 101–106.

(76) Hutchinson, J. S.; Reinhardt, W. P.; Hynes, J. T. *J. Chem. Phys.* **1983**, 79, 4247.

(77) Sacchi, M.; Wales, D. J.; Jenkins, S. J. *J. Phys. Chem. C* **2011**, 115, 21832.